Journal of Engineering and Engineering Technology

PRODUCTION AND CHARACTERIZATION OF ALUMINA NANOPARTICLES FROM GIRO CLAY VIA ACID LEACHING WITH SOL GEL METHOD

Balogun S.O [1*], Yaro S.A [2], Abdulwahab M. [3] and Kasim A. [4]

[1*] Nigerian College of Aviation Technology, Zaria.
[2,3,4] Department of Metallurgical and Materials Engineering, Ahmadu Bello University, Zaria

ABSTRACT

Alumina nanoparticles were synthesized from locally available high alumina clay, obtained from Giro in Kabbi State, through acid leaching with sol-gel method. The clay was leached with hydrofluoric acid and the aluminous solution produced was used as precursor to synthesis nanoparticles through sol gel process. The composition and structure of the clay and the particles produced were characterized using Fourier Transform Infrared (FTIR), X-ray diffraction and fluorescence Spectroscopic techniques, Scanning Electron Microscopy (SEM) and Transmission Electron Microscopy (TEM). From the analyses, the clay sample was observed to be high in alumina and predominantly Kaolinitic in nature. During the sol-gel process, effective flocculation was obtained at slightly alkaline pH range (7.6 to 8.0) and a relative moderate temperature of $80°C$. The result also shows that the aging time of the gel affected the size of the particles produced during the process, and the particles are mainly nano-alumina.

Correspondence:
*balogunsherifola@gmail.com, yaroaliyu@yahoo.com, mabdulwahab@abu.edu.ng, akasim@abu.edu.ng

1.0 INTRODUCTION

Alumina is an important ceramic material utilized in wide range of applications due to its unique characteristics, viz., high hardness and modulus, excellent dielectric properties, refractoriness and thermal properties (Abyzov, 2019). Alumina powder with average particle size of less than 100nm is referred to as alumina nanoparticles (Hu, Onyebueke and Abatan, 2010). Nanoparticles possess improved properties when compared to bulk materials due to their high surface to volume ratio (Chatterjee and Mallick, 2013). Alumina nanoparticles is particularly attractive in the development of nanocomposites; which are contemporary materials in the aerospace and automotive industries. However, the development of cost effective means of producing Nano alumina material remains a challenge of the industry (Behera, Sarkar and Bhattacharyya, 2016). Although Nano alumina can be synthesized from aluminium bearing chemical compounds, such as aluminium alkoxides precursors, the production of Nano alumna directly from aluminous minerals such as bauxite (Manirasakan *et al.*, 2009) is more sustainable. However, high grade bauxite is not commonly available in most part of the world, hence industries and researchers are exploring the production of alumina from other available aluminous minerals

(Abdulwahab and Al-Sindy, 2006; Al-zahrani and Abdul-majid, 2009; and Olaremu, 2015).

Clays are earthy minerals which comprises mainly of aluminosilicates in fine grains. Alumina can be extracted from clay mineral for industrial use. Acid leaching is the most common method utilized for the extraction of alumina from clay, mainly because of its flexibility in ore grade requirements and low cost implication (Al-Zahrani and Abdul-Majid, 2009; Pinna, Barbosa and Rodriguez, 2017). A common definition of high alumina clay was by W.D Keller in 1963; clays with alumina content of above 39.5% was considered to be of high alumina (Coelho *et al*., 2020). It is expected that a high alumina clay, will translate to a relative higher alumina extraction yield when leached. There is a reasonable amount of clay resource in the northern region and many parts of Nigeria, hence it's worthy to explore their potential industrial application. There is a relatively large deposit of clay in *Giro* in Kebbi State and the community at times use it for burnt clay works which is an indicator for its suspected refractoriness and high aluminium oxide content (Sabtendra *et al*., (2014).

Acid leaching is frequently employed in the extraction of valuable metals from ores. This technique is mainly attractive not only because of its effectiveness but for its low energy requirement, ore grade flexibility, low cost and eco-friendly nature (Hebbache *et al* 2009; Ajemba and Onukwuli 2012). The dissolution of clay mineral can be carried out using leaching agents such as hydrofluoric acid, hydrochloric acid, sulphuric acid or nitric acid (Ajemba and Onukwuli 2012; Pinna, *et al*., 2018).

Nanoparticles are produced through a variety of techniques, such as precipitation process, mechanical milling and sol-gel process. Among these, sol-gel processing technique is frequently used to produce nano-structured material because the process is controllable, relatively cost effective and can guarantees clean product (Zhang, 2004; Rogojan, Andronoscu, Ghitulica, and Vasile (2001) & Manivasakan *et al*. 2013).

Sol gel process is a wet chemical solution deposition technique, which involves the production of colloidal suspension (sol) from a precursor, which is condensed into a new phase (the gel). The gel can be dried. The size and morphology of the particles in this process depends on factors such as concentration of the original solution, pH of the solution and the heat treatment time and temperature. Nanoparticles in a system becomes stable at pH where the zeta potential is high (Nidhin, 2008). Heating temperature and time during the aging process can affect both crystal phase and size of the particles (Mosoudch *et al*. 2011).

Production of alumina nanoparticles from clay through a simple route is of economic importance as this would mean a reduced raw material cost. Therefore, the aim of the present study is to investigate the possible production of alumina nanoparticles from local high alumina clay using sol-gel method. The effect of aging time on particle size was also studied during the synthesis.

2.0   MATERIAL AND EXPERIMENTAL PROCEDURE

Clay sample used in this investigation was sourced from *Giro* locality

(latitude/longitude:11°45'58"N / 4°10'49"E) in Kebbi State, a northern region of Nigeria. The reagents used during the investigation were sodium hydroxide, hydrofluoric acid, acetic acid and Cetyl trimethyl ammonium bromide (CTAB). The CTAB was purchased from Sigma-Aldrich Co., Ltd and all other reagents were purchased from Fisher Scientific Ltd. All reagents involved were of analytical grade and utilized without further purification.

Synthesis of Alumina Nanoparticles

50g of high alumina high alumina clay was heated in a muffle furnace at the rate of 15°C/min. up to a temperature of 800°C, in order to make it more susceptible to acid dissolution. This was held at this temperate for 10mins, after which it was leached with 200ml of 2Molar hydrofluoric acid solution. The resulting solution was stirred for 1 hour while the temperature was maintained at 80°C. To allow for the precipitation of non-aluminous hydroxides, the pH of the solution was adjusted to 6 with NaOH (6Molar) solution. The resulting product was filtered and the filtrate was utilized as the sol. In the sol-gel process, using the sodium hydroxide solution, the pH of the precursor was adjusted to a value of 12 to keep the aluminous hydroxide well in solution and CTAB was added as surfactant. The solution was stirred vigorously at 80°C and acetic acid was added in drops until flocculation occurred. This was obtained at a pH range of about 7.6 to 8.0. The gel was allow to age before it was dried at 110°C for 1 hour.

To study the effect of aging time on the particle size, aging for 3, 6 and 9 hours was experimented. The particles were washed with water to remove any salt and surfactant before finally rinsing with ethanol and dried. Samples produced at the optimum condition was fired at 900°C in a muffle furnace for 6 hours and de-agglomerated using a ball mill with a 10:1 weight ratio of the balls to the powder, and rotated at 550 rpm. for 1 hour.

Characterization

The composition of the clay and nanoparticles produced were investigated using XRD, XRF and FTIR analytical techniques. The XRF was carried out on a Mini PAN anlytcal spectrometer (PW 4030 X-ray) while the XRD was done on a Philips X-ray Diffractometer (DXR 3000).The FTIR spectrums were obtained using an Agilent infrared spectrometer (Agilent 4500 series) using KBr pellets. The morphology of the nanomaterial was observed using a Phenom ProX scanning electron microscope and the high resolution TEM image was obtained with a JEOL JEM2100F Electron Microscope.

3.0 RESULTS AND DISCUSSION

XRF Analysis Result

The results of XRF analysis of the as-received clay and nano-particles is shown in Table 1 and 2 respectively.

Table 1: XRF chemical composition of as-received clay mineral

Oxide	Al2O3	SiO2	Fe2O3	TiO	CaO	MgO	Others
%Weight	42.031	49.877	6.272	1.205	0.042	0.089	0.364

Table 2: XRF chemical composition of the synthesized particles from clay

Oxide	Al2O3	SiO2	TiO	CaO	MgO	Fe2O3	Others
%Weight	90.8	7.487	0.24	0.0023	0.014	0.48	0.977

The XRF analysis of the clay sample reveals that the amount of Al_2O_3 present is about 42%. This amount is more than the theoretical value of alumina in Kaolinite, hence it's a clay of high alumina content. The result in Table 2 shows that the alumina content in the particles produced is 90.8%. Hence, high amount of silica and other oxides were leached from the clay during the acid treatment and the percentage of alumina content in the product has been enhanced. Ogbonnaya *et al.*, (2018), reported extracting about 94% by wieght of alumina when *Aku* clay was leached with hydrochloric acid.

XRD Analysis Result

The X-ray diffraction patterns of the natural clay sample and nanoparticles produced is presented in Figures 1 and 2, respectively.
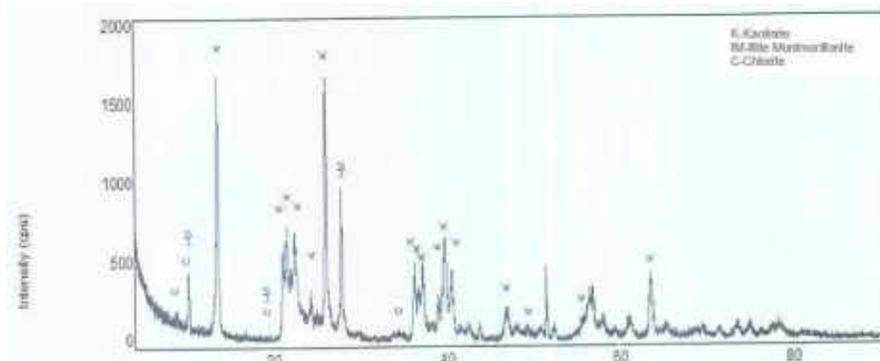

Figure. 1: XRD pattern of as-received clay sample

XRD pattern of the as-received clay showed various crystalline peaks in the sample. The major minerals from the diffractogram peaks obtained when matched with standard stick patterns, corresponds to Kaolinite, in association with illite-montmorillonite and Chlorite. Since the chemical analysis reveals that the specimen is relatively high in alumina, it is suggestive that the chlorite is an aluminium-chlorite.
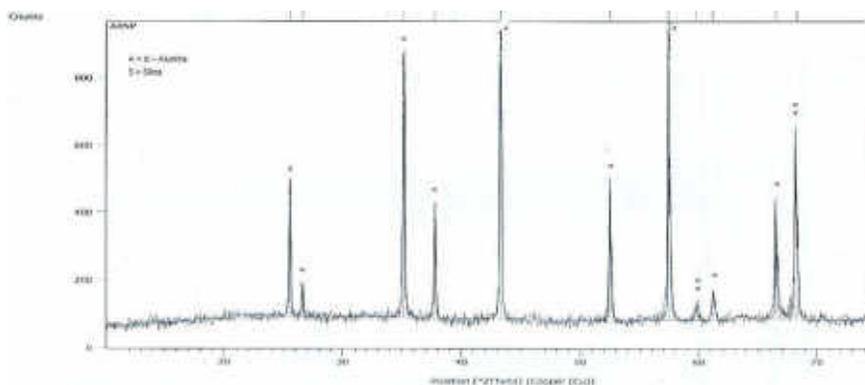

Figure 2:   XRD pattern of the nanoparticles produced form clay through sol-gel route.

From the XRD pattern (Figure 2) of the synthesized particle eleven main reflections were observed at 2 theta angles around 25°, 26°, 35°, 37°, 43°, 52°, 57°, 59°, 61°, 66°, and 68°.

These peaks were indexed to alumina and silica, which has phase scores of 90% and 10% respectively. This agrees with the outcome of the XRF analysis in respect to the quantity of alumina.

FTIR Analysis Result

The FTIR spectra of the as-received clay and the synthesized nanoparticles are presented in Figures 3 and 4 respectively.
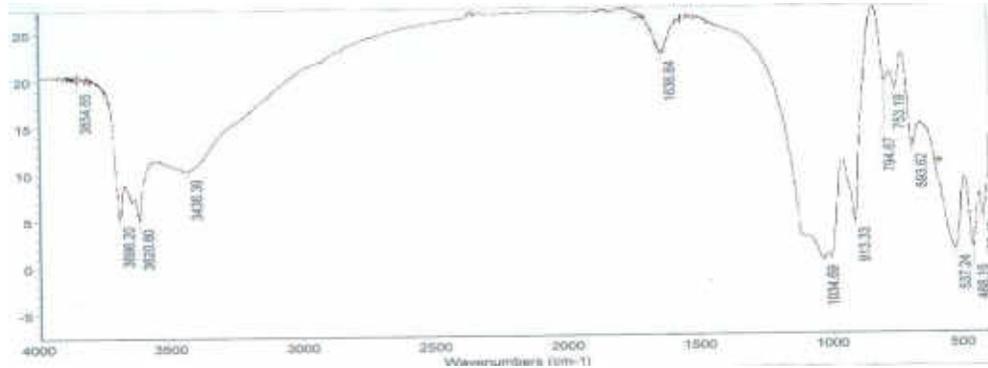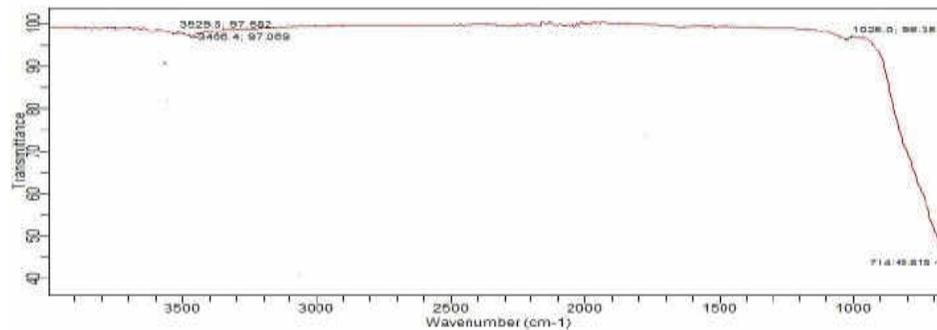

Figure 3: FTIR spectrum of the as-received clay

Figure 4: FTIR spectrum of the synthesized nanoparticle from clay.-received clay

The infrared spectrum of the clay sample shows a relatively broad band absorption, as indicated in Figure 4. The main functional group obtained from this spectrum are -OH stretches (above 1500 wave number), Al-OH and Si-O deformations (in the fingerprint region). The band at 3696, 3660 and 3620 cm^{-1} show frequency peaks of OH stretching, with medium absorbance strength. The peak at $3696cm^{-1}$ is attributed to inner-surface OH stretching and this agrees with $3695cm^{-1}$ reported for kaolin clay by Edomwonyi-Otu *et al.*, (2013). The peak at $3660cm^{-1}$ is assigned to inner-cage OH stretching of kaolinite and this closely similar with $3655cm^{-1}$ reported by Kristo *et al.*, (1997). The main distinction of kaolinite mineral is observed with the OH stretching absorption. Inner-hydroxyl group is obtained at $3620cm^{-1}$ which is typical of a high amount of Al-OH in the octahedral sheet and agrees with 3620 and $3619cm^{-1}$ reported by Mgbemena *et al.* (2013) and Vahur *et al.* (2016) respectively. The bands near $1030cm^{-1}$ Using to Si-O planar stretching common with

kaolinite. The absorption near 913 cm^{-1} is due to Al-O-H vibrations found in kaolinite. The doublet at 770 and 750cm^{-1} are indicative of Al-O-Si and Si-O-Si inner surface vibration respectively (Ritz *et al*., 2011 and Saikia *et al*., 2010).

The absorption peak band around 3650-3360 cm-1 and weak peaks near 998 and 912cm^{-1} is indicative of illite-montmorillonite mixed-layer clay (Ritz *et al*., 2011). These bands are associated with stretching and bending mode of hydroxyl groups and Si-O and OH stretching respectively. The bands at 846 and 805cm-1 are probably indicative of Al-Mg-OH deformations. The absorption band located around 429 and 468 wavenumbers is characteristic of Al-O and FeO absorptions (Vahur *et al*., 2016). The existence of Kaolinite and illite-montmorillonite was confirmed by the representative absorption spectra of the sample clay.

On the IR spectra of the synthesized particles presented in Figure 4, peaks near 3466.4cm^{-1} and 714.45cm^{-1}, correspond with vibration signals attributed to alumina. This result is also in agreement with the spectrum of alumina as reported by Manivasakan *et al*., (2009) and Varghese *et al*., (2014). The broadband centered at 3250-3500 cm^{-1} results from the vibration bands of the hydroxyl group. The absorption peak near 1026 cm^{-1} is assigned to the Si-O-Si asymmetric stretching vibration (Vahur *et al*., 2016; Feifel and Lisdat (2011) and Manivasakan *et al*., 2009).

SEM and TEM Results.

The surface morphology of the nanoparticles produced from the high alumina clay at different aging time, as shown by scanning electron microcopy images are presented in Figures 5(a–d).
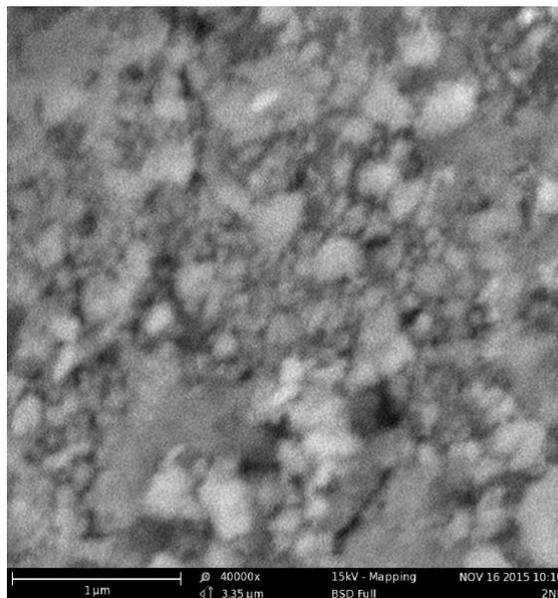

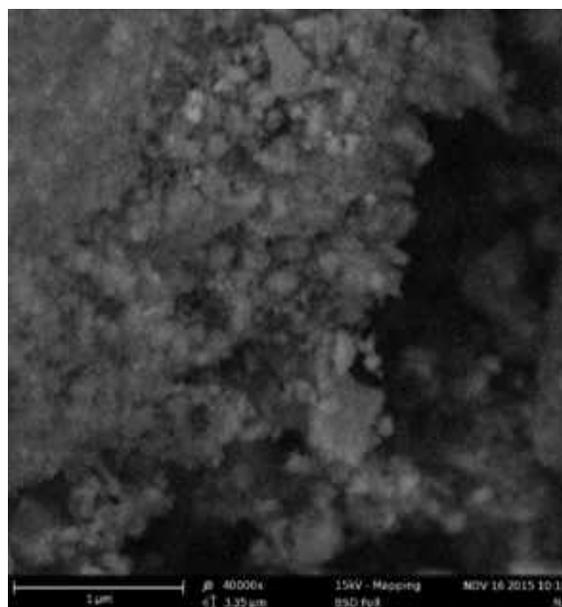*Figure 5a: SEM image of nanoparticles produced from clay through sol-gel route (Aged for 3hrs)*

Figure 5b: SEM image of nanoparticles produced from clay through Sol-gel process (Aged for 6hrs)

Figure 6: TEM Image of Nanoparticle produced from clay through Sol-gel process (aged for 6hrs) and calcined at 900 °C
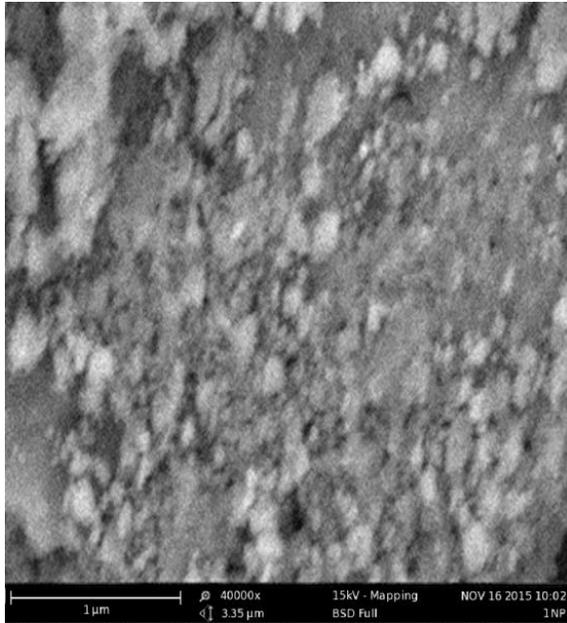
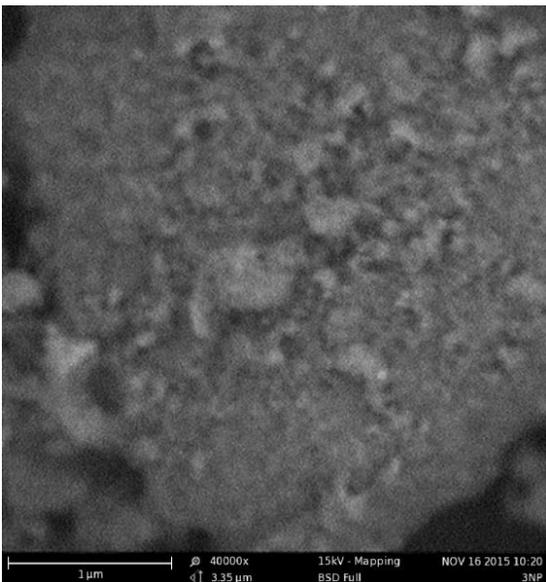*Figure 5c: SEM image of nanoparticles produced from clay through Sol-gel Process (Aged for 9hours)*

Figure 5d: SEM image of nanoparticles produced from clay through Sol-gel Process (aged for 6hour), Ball-milled and Calcined

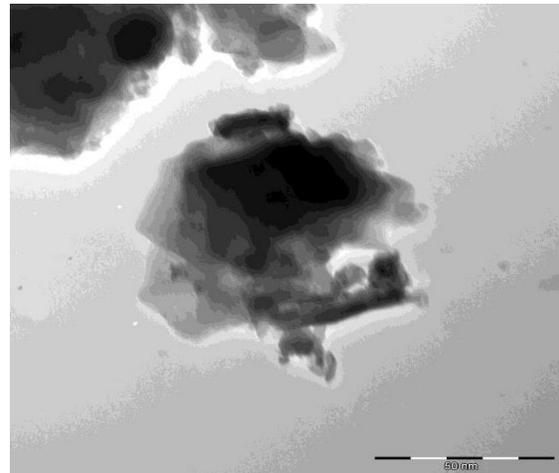The SEM micrographs (Figures 5a-d) revealed that the particles are fine and are mostly globular. From the SEM images, a reduction in the particle sizes was observed as the aging time of the gel was increased from 3 hours to 6 hours and then it decreased when aging was for 9 hours. The average particle sizes was estimated, using imagery analysis software, to be 126 nm, 97 nm, and 112 nm for the samples aged for 3 hours, 6 hours and 9 hours, respectively. The least particle size was observed when the gel was aged for 6 hours. This trend may be explained using Ostwald ripening phenomenon (Redmond *et al.*, 2004); at a lower ageing time (3 hours in this case), stable nucleation of particles was not formed before the gel was dried, while stable nucleation was formed when the sol was aged for 6 hours. At a higher aging time (9 hours), small sol particles dissolved and redepositeded on the surface of larger sol particles to form a much larger particles. The trend of this result agrees with works by Bogdanoviciene *et al.*, (2007) and Shahini et al., (2011). The average size of the calcined particles, using imageJ® software, was determined to be 93nm. The morphology of the nanoparticles synthesized presents a

regular repetition of nearly spherical grains with some larger and agglomerated particles in some cases. The TEM capture of some particles (Figure 6), also indicate that the morphology of the nanoparticle is near spherical.

4.0   CONCLUSIONS

The following conclusions were drawn from this investigation:

1. The *Giro* clay sample collected is mainly Kaolinitic in nature and contains a relatively high percentage of alumina (42%). Hence it is a high alumina clay. Associated minerals such as illite-montmorillonite and chlorite was also observed in the clay.

2. Alumina rich particles in the nano sized range can be synthesised from this clay by leaching with concentrated HF acid and sol-gel process carried out under a moderate temperature, pH value and aging time.

3. The aging time of the gel during the sol-gel process has effect on the size of the particles produced. As the aging time was increased the particle size reduced up to a point before growing larger.

REFERENCES

Abdulwahab, A, Al and Al-Sindy, S.I. (2006). Alumina Recovery from Kaolinitic Clay by Hydrochloric Acid Route. *Iraqi Bulletin in Geology and Mining*. Vol. 2 (1).

Abyzov, A. M, (2019). Aluminium oxide and alumina ceramics (review). Part 1. Properties of Al_2O_3 and commercial production of dispersed Al_2O_3. *Refract Ind. Ceram* 60, 24-32.

Ahmadi, M., Ghasemi, M.R and Rafsanjani. (2011). Study of different Parameters in TiO2 Nanoparticles Formation. *Journal of Material Science and Engineering*. Vol 5 pp. 87-93.

Ajemba, R. O., and Onukwuli, O. D., 2012. Process optimal of sulphuric acid leaching of alumina from Nteje clay using central composite rotatable design. *Int. Multidiscip. Sci. Eng*. 3 (5).

Alexminerals. (2017). High Alumina Clay. Retrieved from www.alexminerals.com/high-alumina-clay.php.

Al-zahrani, A.A and Abdul-majid (2009). Extraction of Alumina from Local Clay by Hydrochloric acid Process. *JKAU: Engineering and Sciences.* Vol 20 (2) pp 29-41

Behera, P. S, Sarkar, R., and Bhattacharyya, S., (2016). Nano Alumina: A Review of the powder Synthesis Method. Interceram. *International Ceramic Review,* 65, pp10-16. http://doi.org/10.1007/BF03401148.

Chatterjee, S., and Mallick A.B. (2013). Challenges in manufacturing aluminium based metal matrix nanocomposite via stir casting route. *Material science forum*. 736, pp. 72-80.

Coelho, C. V. S., Moreira, C. A., Rosolen, V., Bueno, G. T., Salles, J., Furlan, L. M., and Govone, J. S., (2020). Analysing clays (Brazil) using electrical resistivity topography (ERT). *Pure and Applied*

Geophysics, 117, 3943-3960.

Edomwonyi-otu, L, Aderemi, O. B., Ahmed, A. S., Coville, N and Maaza, M. (2003). Influence of Thermal Treatment on Kankara kaolinite. *Opticon* 1826. 15 (5). Pp 1-5. doi: http://dx.doi.org/10.5334/opt.bc.

Egbuna S.O., Mbah G. O. and Mbah-Iroulo. (2018). Optimization and process modeling of the extraction of alumina from Aku clay by hydraulic Acid leaching. *American Journal of Engineering Research*, vol. 7 (11), pp 158-169.

Habbache, N., Alane, S., Djerad, L., and Tifouti, 2009. Leaching of copper oxide with different acid solution. *Chem. Eng. J.* 221 (4), 1-2.

Hu, H., Onyebueke, L and Abatan, A., (2010). Characterization and Modeling Mechanical Properties of Nanocomposite-Review and Evaluation

Keller W. D (1963). The Origin of High-Alumina Clay Minerals-A Review. *Twelfth National Conference on Clays and Clay Minerals,* pp.129-144

Kristo, J, Frost R. L, Felinger, A and Mink, J. (1997). FTIR Spectroscopic study of intercalated kaolinite. *Journal of Molecular Structures*. Vol. 410-411. Pp 119-122.

Manirasakan, P., Rajendra V., Rauta, P. R., Suhu, B. B and Panda, B, K. (2009). Direct synthesis of nanoalumina from natural bauxite. *Advanced materials Research*, vol.67. pp 143-148.

Manirasakan, P., Rajendra V., Rauta, P.R., Suhu, B. B and Panda, B, K. (2009). Direct synthesis of nanoalumina from natural bauxite. *Advanced materials Research*, vol.67. pp 143-148.

Manivasakan, P., Karthik, A., and Rajendvar,V. (2013). Mass production of Al_2O_3 and ZnO_2 nanoparticles by hot-air spray pyrolysis. *Powder technology (Elsevier)*. Vol.234 pp 84-90. doi 10.1016/j.powtec.2012.08.028.

Mgbemena, C. O., Ibekwe, N. O., Sukamar, R., and Menon, A. R. R. (2013). Characterization of kaolin intercalates of oleochemical derived from rubber seed (Hevea brasiensis) and tea seeds (camellia sinensis) oils. *Journal of King Saud University – science*. 25. Pp 149-155.

Mosoudch, A., Mohammad, R. G. and Hassan, H. R. (2011). Study of different Parameter in TiO2 Nanoparticles Formation. *Journal of Material Science and Engineering*. Vol.5, pp. 87-93.

Nidhin M, Indumathy R, Sreeram, K,J & Nair, B.U. (2008). Synthesis of iron oxide nanoparticles of narrow size distribution on polysaccharide templates. *Bull. Mater. Sci.*, vol. 31 (1) pp. 93-96.

Olaremu, A. G. (2015). Sequential leaching for the production of Alumina from Nigerian Clay. *International Journal of Engineering Technology, management and Applied Sciences. Vol. 3 Iss 7.*

Pinna, E. G., Barbosa, L. I., Suarez, D. S., and Rodriguez, M, H., 2018. Kinetic study of dissolution of metalkaoline with hydrofluoric acid. *Indian J. Chem. Technol.,* 25, 287-293.

Redmond, P. L, Hallock, A. J, and Brus, L. E (2005). Electrochemical Ostwald

Ripening of Colloidal Ag Particles on Conductive Substrates. *Nano Letters*, vol. 5 (1). Pp. 131-135.

Ritz, M., Plevova, E and Vaculikora, L. (2011). Application of infrared spectroscopy and chemometric methods to identification of selected minerals. vol. 8 No. 1 (161). Pp. 47-58.

Sebtendra R., Nugroho. S and Umardani., Y. (2014). Physical characterization of alumina (Al_2O_3) based refractory application on induction furnace lining. *Jurnal teknik mesin s-1*, vol 2 (1), pp 77-84.

Sekunowo, O.I., Durowaye, S. I. and Lawal, G. I. (2015). An Overview of Nano-Particles Effect on Mechanical Properties of Composite. *International Journal of Mechanical, Aerospace, Industrial Mechatronic and Manufacturing*. Vol. 9. (1).

Shahini, S., Askari, M and Sadrnnezhaad S. K. (2011). Sol- Gel Synthesis and Aging Effect on Highly Crystaline Anatse Nanopowder. *Bulletin of Material Science. (Springer)*. vol 34, Iss.6, pp 1186-1195.

Vahur, S., Teearu, A., Peets, P., Joosu, L., and Leito, I. (2016). ATR-FT-IR Spectra collection of conservation materials in the extended region of 4000-80 cm^{-1}. *Analythical and bioanalytical chemistry*. Vol. 408 (13). Pp. 3373-3379.

Zhang, L. (2004) Preparation of multi component ceramic nanoparticles. Retrieved from:

www.mse.eng.ohiostate.edu/fac_staff/faculty/verweij.